Journal of Cleaner Production 350 (2022) 131541

Contents lists available at ScienceDirect

Journal of Cleaner Production

journal homepage: www.elsevier.com/locate/jclepro

Green synthesis of ZnO nanoparticles using polyphenol extracts from pepper waste (Capsicum annuum)

Mercedes Jiménez-Rosado [a,*], Andrea Gomez-Zavaglia [b], Antonio Guerrero [a], Alberto Romero [a]

[a] Department of Chemical Engineering, Higher Polytechnic School, Faculty of Chemistry, Universidad de Sevilla, Seville, Spain
[b] Center for Research and Development in Food Cryotechnology (CCT-CONICET La Plata) RA-1900, Argentina

ARTICLE INFO

Handling editor: Prof. Jiri Jaromir Klemeš

Keywords:
Capsicum annuum
Green synthesis
Nanoparticles
Pepper
Polyphenols
Zinc oxide

ABSTRACT

The nanoparticles (NPs) synthesis poses an environmental problem: the formation of other toxic substances. An eco-friendlier alternative method based on the use of polyphenolic extracts is gaining interest due to their potential to reduce metal salts for the formation of NPs without toxic products. Thus, the main objective of this work was to obtain zinc oxide (ZnO) NPs from pepper extracts rich in polyphenols. To this end, the polyphenol extraction process was set-up using a response surface analysis of the different parameters involved (*i.e.* temperature, extraction time, amount of pepper and solvent used, type of solvent and part of the pepper used -whole fruit, pulp or waste-) in terms of total polyphenol content (TPC) and antioxidant activity of the extracts. The optimal extracts were used to synthesize ZnO NPs by colloidal precipitation, which were further characterized through X-ray diffraction, scanning electron microscopy, Fourier-transform infrared spectroscopy and antioxidant activity tests. In addition, the green NPs were compared with those obtained from chemical reagents. The green synthesized NPs were purer (100 and 88% ZnO content for green and chemical NPs) and smaller (24–43 and 35–70 nm for green and chemical NPs). The results show the great potential of pepper polyphenol extracts to obtain ZnO NPs by a green synthesis, being a great contribution to environmental sustainability.

1. Introduction

The UNE-CEN ISO/TS 80004–2:2017 standard defines nanomaterials as those with a scale of characteristic external lengths (grain size, particle diameter, layer thickness, etc.) under 100 nm ("UNE-CEN ISO/TS 80004–2:2017. Nanotecnologías. Vocabulario. Parte 2: Nano-objetos," 2017). In this context, nanomaterials can be classified according to the lengths that meet this requirement: nanoparticles (3 dimensions <100 nm), nanofibers (2 dimensions <100 nm) and nanolayers (1 dimension <100 nm). The structure of nanomaterials is composed of atoms rearranged in specific ways, which grant them unique characteristics that differ from those of the materials themselves (Murty et al., 2013). Generally, this change in size can modulate optical, catalytic, electronic, magnetic and mechanical properties (Saleh, 2020). In addition, their extremely low surface area allows them to be incorporated in a material at a very low amount with excellent percolation (Mariano et al., 2014).

In this way, nanoparticles (NPs) have changed the perception of many industries (Guozhong, 2004). They have begun to be used on various applications, obtaining unexpected results. Among such applications, NPs have great potential (Gobierno de España, 2021) in food (Jamróz et al., 2019; Kharazmi et al., 2020; Wrona and Nerin, 2020), textiles (Leon et al., 2019), pharmaceuticals (Niora et al., 2020), medicine (Tang et al., 2020), electronics (Dawood et al., 2020) and agriculture (Pérez-Labrada et al., 2020).

NPs can be synthesized by different physical and chemical methods (Talam et al., 2012). Among them, colloidal precipitation is the most widely used method, due to the ease modulation of the final NPs characteristics (Handal et al., 2021; Nguyen et al., 2021; Petcharoen and Sirivat, 2012; Saleem et al., 2021). This method starts from the mixture of a precursor and a reducing agent, leading to a product further subjected to a heat treatment (calcination) for obtaining NPs. The characteristics of these NPs can be fine-tuned by setting up the concentration and ratio of the precursor and reducing agent, reaction pH and calcination temperature (Chen et al., 2008). From a chemical viewpoint, the reducing agent is usually a hydroxide that allows –OH groups to join the cation of the precursor and form an intermediate hydroxide. Such intermediate can generate the NPs under thermal conditions. However, the use of these reducing agents often generates toxic materials (unreacted starting materials, excess reagents, and by-products resulting from side reactions or degradation pathways) (Sheldon, 2005) and

* Corresponding author. Department of Chemical Engineering, Universidad de Sevilla, Spain.
E-mail address: mjimenez42@us.es (M. Jiménez-Rosado).

https://doi.org/10.1016/j.jclepro.2022.131541
Received 10 December 2021; Received in revised form 6 March 2022; Accepted 24 March 2022
Available online 27 March 2022

makes the final product more expensive, limiting the progress of science and also contributing to the carbon footprint (Prabhu and Poulose, 2012). In addition to limiting their use in applications such as medicine, pharmacy or food, since the presence of these materials could be harmful to humans (Varma, 2012).

In order to overcome these drawbacks, using polyphenols as reducing agents could lower manufacturing costs, also providing more eco-friendly methods (Debnath and Gupta, 2018). In this way, the use of these reagents can maximize the desired products and minimize by-products (Li, 2016; Li and Trost, 2008). Polyphenols are compounds naturally occurring in plants (Parveen et al., 2016), characterized by the presence of more than one phenol group per molecule (in general, each molecule presents from 2 to 14 –OH groups, which is correlated with their antioxidant activity) (Gironi and Piemonte, 2011). Due to the large availability of –OH groups, polyphenols can act as reducing agents in the synthesis of NPs, also preventing the generation of toxic secondary products (Agarwal et al., 2017). Thus, they allow an efficient synthesis due to their selectivity and economic in atom count (Trost, 1991). These polyphenols can be easily extracted from plants by solubilizing them in polar solvents, such as alcohols or water (Prado et al., 2021). Nevertheless, it is important to control the extraction parameters (*i.e.*, temperature, time, concentration, etc.) to optimize the amount of polyphenol groups extracted and their antioxidant activity, which will determine their ability to reduce the precursors to obtain NPs (Özbek et al., 2020; Pietrzak et al., 2014). This approach has been employed to synthesize NPs from different plant extracts, such as *Glycyrrhiza Glabra* (Vivekananth et al., 2021), *Calendula officinalis* (Nematollahi et al., 2021) and *Phoenix Dactylifera* (Abdullah et al., 2020; Rajeswari et al., 2021).

Pepper (*Capsicum annuum*) has a large content of polyphenols with a high antioxidant activity (Marín et al., 2004; Arthur Niamke and Soro, 2021). Thus, pepper (1.4 g/kg) has a higher polyphenols content than asparagus (1.2 g/kg) and chickpeas (0.10 g/kg), matching black beans and eggplant (Almonacid, 2016). The global production of pepper was approximately 42 million tons in 2019 (Food and Agriculture Organization of the United Nations, 2021a), and 12% of these are wasted (5 million tons) due to poor quality (deformations of the pepper or stains on them caused by high temperatures, storms or lack of nutrients during harvest) and inedible parts (*i.e.*, seeds, peduncles, etc.) (INTAMinisterio de Agricultura de Chile, 2018). These discards reduce the economic production performance and costs since they have to be disposed. Furthermore, the organic composition of pepper implies a significant environmental impact, having a large carbon footprint (vegetables as a whole lead to *ca.* 6% which is related to the waste plan required) (Food and Agriculture Organization of the United Nations, 2013). Therefore, the use of pepper wastes as source of polyphenols in the synthesis of NPs could be a smart alternative to add them value, also promoting their circular economy and reducing environmental pollution. Thus, the lower carbon footprint and price generated by the green method is justified by changing the use of chemical reducers for natural reducers that are waste, as is reflected in different previous works (Abomuti et al., 2021; Debnath and Gupta, 2018; Feijoo et al., 2018).

Therefore, the main objective of this work was to evaluate the use of pepper polyphenol extracts for the synthesis of zinc oxide (ZnO) NPs. To achieve this goal, the optimization of the polyphenol extraction process was firstly evaluated in terms of the total polyphenol content and antioxidant activity. Then, in order to support the suitability of the green synthesis of NPs, different ZnO NPs were obtained using the optimal polyphenol pepper extracts and compared with those synthesized with the "traditional" chemical method in terms of purity, crystallinity, size and antioxidant activity.

2. Materials & methods

2.1. Materials

Italian sweet peppers (*Capsicum annuum*) were chosen as they are the most consumed worldwide (Food and Agriculture Organization of the United Nations, 2021b). They were obtained from the local market (Seville, Spain). All the other reagents (*i.e.*, methanol, ethanol and zinc chloride) were provided by Sigma Aldrich (USA).

2.2. Polyphenol extraction

Firstly, the peppers were grounded using an Ironmix kitchen robot (Cecotec, Spain). This grinding improves the posterior interaction of the pepper components with the solvent during the extraction. The extraction was carried out by magnetic stirring (1000 rpm). Thus, the grounded pepper (<1 mm) was mixed and stirred with a solvent (methanol, ethanol or distilled water) for a given time (15, 30 or 45 min) at a selected temperature (20, 35 or 50 °C). Different pepper:solvent ratios (1/1, 2/1, 1/2, 4/1, 1/4) were also evaluated. Finally, the crude extract was centrifuged in a Sigma 3–18K centrifuge (Germany) at 15,000 rpm and 10 °C for 10 min to eliminate insoluble impurities and obtain the refined extract rich in polyphenols (supernatants). The whole, pulp and waste parts of the pepper were analyzed separately. For the whole, all the pepper was used as purchased. In the case of the pulp, the fleshy part of the pepper was used and for the rest, the peduncle, stem and disposable parts due to brown spots (overripe) were taken.

A Box-Behnken design (BBD) was used to optimize the extraction conditions. Briefly, the independent variables (X) were evaluated in pairs (temperature-time and pepper amount-solvent volume), according to their affinity, to determine their individual and joint influence on the dependent variables (Y). The latter variables (*i.e.*, total polyphenol content and antioxidant activity) act as responses in the BBD experiment. The models were chosen using the Design-Expert software (version 11, Science Plus, Netherlands). F-value and a confidence level of 95% (p-value <0.05) were taken into account to analyze the data and the coefficients. Thus, the model was determined only with the significant parameters that generated a lack of fit without significance ($p > 0.05$) and precision greater than 4.

2.3. Polyphenol characterization

2.3.1. Total polyphenol content (TPC)

The total polyphenol content was determined by Folin-Ciocalteu's method (Noreen et al., 2017). Firstly, 50 μL of each extract were mixed with 2 mL of distilled water and 250 μL of 1N Folin Ciocalteu's phenol for 8 min. Later, 750 μL of 20 wt% Na_2CO_3 and 950 μL of distilled water were added. The absorbance of the obtained solutions was measured at 765 nm in a spectrophotometer (Genesys-20, Thermo Scientific, USA) after 30 min of maturation in the absence of light. Gallic acid was used as a reference, and the results were expressed as g gallic acid equivalent (GAE) per mL of extract.

2.3.2. Antioxidant activity

The antioxidant activity was evaluated using the phosphomolybdate (PPM) method (Abdullah et al., 2020). A volume of 2 mL of extract was mixed with 2 mL of PPM reagent (Na_2HPO_4 28 mM, $(NH_4)_6Mo_7O_{24}{\cdot}4H_2O$ 4 mM and H_2SO_4 0.6 mM) for 90 min in a water bath at 95 °C. The absorbance of each sample was measured in a spectrophotometer at 699 nm, using Gallic acid as a reference to calibrate. The results were represented as g GAE/mL extract.

2.4. Nanoparticles' synthesis

Nanoparticles (NPs) were synthesized through colloidal precipitation (Chen et al., 2008). The green synthesis of NPs was carried out using

zinc chloride ($ZnCl_2$) as the precursor and the optimal polyphenol extracts as reducing agents. It is worth mentioning that zinc chloride was used as a cheap reactant widely used in literature (Pourrahimi et al., 2014; Shankar and Rhim, 2019). A volume of 20 mL of each reagent (precursor and reducing agent) were mixed for 2 h at 50 °C to favor the reaction, using different concentrations (8, 20 and 40 mg/mL) and ratios (1:1, 1:2 and 2:1). The precipitate obtained was filtered and washed twice with distilled water, furtherly dried at 100 °C for 8 h, and subsequently calcined at 500 °C for 4 h to obtain ZnO NPs. The predicted mechanism for the formation of ZnO NPs is the following, where zinc chloride (precursor) acts with the polyphenols to form an intermediate compound (zinc hydroxide). This intermediate compound is transformed into zinc oxide thanks to the heat produced in the calcination step:

$$ZnCl_2\ (aq) + 2\ R\text{–}OH\ (aq) \rightarrow Zn(OH)_2\ (s) + 2\ R\text{–}Cl\ (aq)$$

$$Zn(OH)_2\ (s) + heat \rightarrow ZnO\ (s) + H_2O\ (v)$$

For comparative purposes, ZnO NPs were also chemically synthesized following the same protocol but using sodium hydroxide (NaOH) as the reducing agent instead of the polyphenol extracts (Chen et al., 2008). Thus, the same precursor concentrations (8, 20 and 40 mg/mL) and precursor:reducing agent ratios (1:1, 1:2 and 2:1) were used.

Finally, the yield of the different synthesis process was obtained by the ratio between the amount of expected nanoparticles (calculated mathematically through the stoichiometry of the proposed reaction) and the nanoparticles obtained.

2.5. NPs' characterization

2.5.1. X-ray diffraction (XRD)

X-ray diffraction (XRD) was used to characterize the physicochemical properties of the NPs through a D81 90 powder diffractometer (Malvern Panalytical, Spain). Briefly, X-Ray at 40 kV and 30 mA impacted with a pitch angle of 0.015° and a passing time of 0.1 s on the samples, which rotated at 30 rpm. Apart from the spectrum, the NPs composition, crystallinity index and crystal size were estimated using the DIFFRAC.EVA software (version 8. Bruker, USA).

2.5.2. Transmission electron microscopy (TEM) and energy-dispersive X-ray spectroscopy (EDS)

The nanostructure and size distribution of the obtained NPs were measured by transmission electron microscopy using a Talos S200 microscope (FEI, USA) at 200 kV. For this, the samples were placed on a carbon-coated copper grid. This microscope also allows obtaining energy-dispersive X-ray spectroscopy (EDS) profiles. The images were analyzed using the Image-J software (free software).

2.5.3. Scanning electron microscopy (SEM)

The nanostructure and size distribution of the obtained NPs, as well as their agglomeration, were evaluated by scanning electron microscopy. To this end, the samples were firstly coated with a thin layer (<10 nm) of Pd/Au to improve their conductivity and, thus, image quality. The samples were observed in an EVO electron microscope (Zeiss, USA) with an acceleration voltage of 10 kV. The images were analyzed using the Image-J software (free software).

2.5.4. Fourier-transform infrared spectroscopy (FTIR)

Infrared spectra were recorded to evaluate the chemical structures and interactions of the synthesized NPs. To this end, a Hyperion 100 spectrometer (Bruker, USA) was used in an absorption mode with a DTGS-KBr sensor. The measurements were obtained between 4000 and 400 cm^{-1} with an opening of 4 cm^{-1} and an acquisition of 200 scans. The intermediate compounds have been also evaluated.

Table 1
Total polyphenol content (TPC) and antioxidant activity of extracts obtained using different extraction temperatures and times. Codes were used to model the parameters (−1: minimum value; 1: maximum value). Different letters indicate significant differences ($p < 0.05$).

Temperature (°C)	Time (min)	Temperature code	Time code	TPC (mg GAE/mL extract)	Antioxidant activity (mg GAE/mL extract)
20	15	−1	−1	239.73^{a}	11951.33^{A}
	30	−1	0	260.18^{b}	12768.00^{ABE}
	45	−1	1	262.00^{b}	12391.33^{B}
35	15	0	−1	269.27^{bc}	9321.33^{C}
	30	0	0	267.91^{bc}	9304.67^{C}
	45	0	1	290.18^{c}	12011.33^{ABE}
50	15	1	−1	242.91^{ab}	16034.67^{D}
	30	1	0	275.64^{c}	13841.33^{E}
	45	1	1	256.55^{ab}	12114.67^{A}

2.5.5. Antioxidant activity

The antioxidant activity of the selected NPs was evaluated by the PPM method. Briefly, the NPs were suspended in HCl 1 M at a concentration of 1 mg/mL. The protocol followed was the same as that described in section 2.3.2.

2.5.6. Ultraviolet–visible (UV–Vis) spectroscopy

UV–Vis spectroscopy were carried out in the different samples. For this, the samples were suspended in distilled water (0.1 g NPs in 100 mL distilled water) by ultrasound (30 min) and later, the resulted suspensions were measured in a UV–Vis spectroscope Pharo 300 (Merk, Germany) from 200 to 570 nm.

The band gap energy (E_{gap}) was calculated using Beer-Lambert's law (Heiba et al., 2021). Thus, E_{gap} was calculated as $1240/\lambda_g$, being λ_g the wavelength correspondent to the optical gap. This λ_g can be calculated by elongating the linear part of $(A/\lambda)^2$ vs. $1/\lambda$ relation at $(A/\lambda)^2 = 0$.

2.6. Statistical analysis

The peppers were selected in order to have a representative sample of the market, mixing different peppers in each measure. In addition, at least three replicates were performed for each analysis and system. All the data were reported as average values. Their standard deviation was statistically calculated using an analysis of variance. Tukey's post hoc test with a confidence level of 95% ($p < 0.05$) was performed using the SPSS 18 statistical package (Excel, Microsoft, USA) to evaluate the significant differences, which were reported with different letters.

3. Results & discussion

3.1. Polyphenol extraction

3.1.1. Effect of mixing temperature and time

The extraction of polyphenols from pepper was optimized by setting up the best combination of temperatures and times of extraction. Regarding the extraction solvent, methanol was selected based on the good results demonstrated in previous works for the extraction of polyphenols (Ferchichia et al., 2021; R. and I., 2012; Vijayalaxmi et al., 2015). The pepper:methanol ratio was established at 1:1 with 100 g of pepper and 100 mL of methanol.

Table 1 shows that in general, the higher the mixing temperature, the greater the TPC of the extracts. This effect was also observed for the extraction time, although to a lesser extent. These results indicate a possible interaction between the substrate (pepper) and the solvent (methanol), favored at high temperatures and at longer extraction times. Nevertheless, the antioxidant activity did not show similar behavior, as the highest antioxidant activity was achieved at 50 °C, followed by 20 °C. In addition, an increase in the extraction time improved the

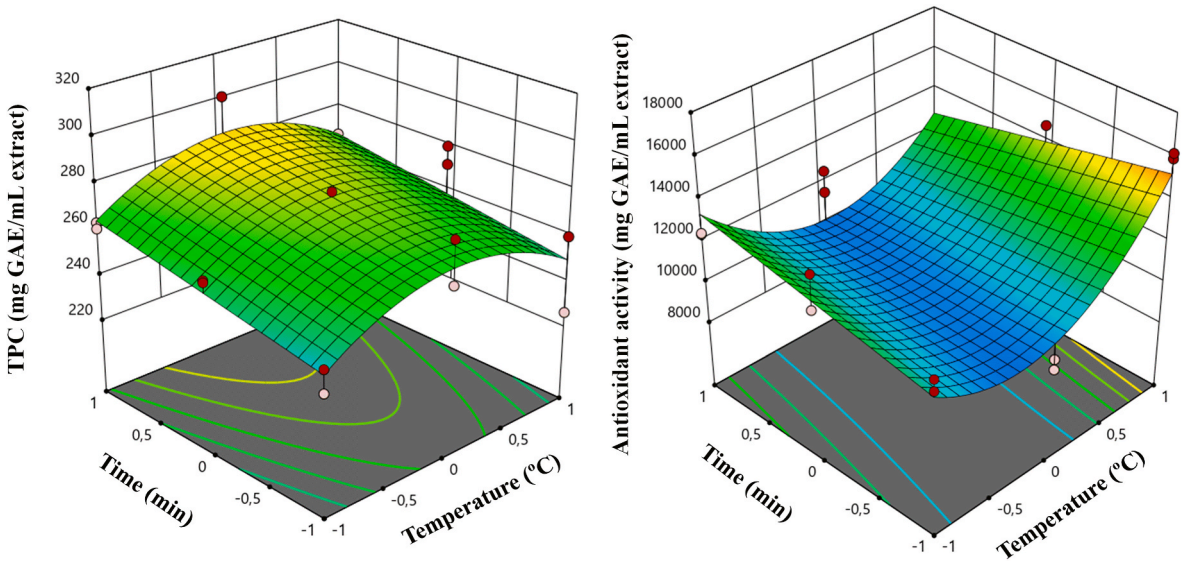

Fig. 1. Response surface of total polyphenol content (TPC) and antioxidant activity of extracts obtained using different temperatures and times of extraction. Temperatures and times are codified from −1 to 1, being the minimum (20 °C and 15 min) and maximum values (50 °C and 45 min), respectively.

antioxidant activity of the extracts at 20 and 35 °C but worsened it at 50 °C. This observation can be explained considering that although higher temperatures (50 °C) may favor the extraction process, the prolonged exposure of polyphenols to those temperatures alters their structures, thereby reducing their antioxidant activity (Casagrande et al., 2018; Spigno et al., 2007).

Quadratic models were used to predict both the TPC and the antioxidant activity responses (Eqs. (1) and (2)) taking into account the temperatures (A) and times (B) employed and avoiding the terms that were not significant. The results are presented in Fig. 1. The response surface graphs indicate that the extraction time did not have a significant influence on the TPC, being included only by the convergence of the model. However, the lack of fit and the value of pure error indicates the good reproducibility of the experimental results (Table S1). In addition, the extraction time affected the antioxidant activity of the extracts to a greater extent, thus creating an antagonistic effect with mixing temperature. On the other hand, quadratic models showed opposite effects of time and temperatures on TPC and antioxidant activity. In other words, the highest TPC values were achieved for the lowest antioxidant activities. This could be due to the fact that the method used to measure TPC does not discriminate between functional polyphenols (which have antioxidant activity) and non functional polyphenols. Therefore, it cannot be concluded by this method that a higher presence of polyphenols corresponds to a higher quality of the extract obtained, which makes it necessary to determine its antioxidant activity. Similar results were obtained by Favre et al. (2020) (Favre et al., 2020).

$$\text{TPC (mg GAE / mL extract)} = 275.8\ (\text{mg GAE / mL extract}) + 1.5\cdot(\text{mg GAE / (mL extract}\cdot^{\circ}\text{C)) A } (^{\circ}\text{C}) + 8.8\ (\text{mg GAE / (mL extract}\cdot\text{min))}\cdot\text{B (min) - 18.9 (mg GAE / (mL extract}\cdot^{\circ}\text{C}^2))\cdot\text{A}^2\ (^{\circ}\text{C}^2) \quad (1)$$

$$\text{Antioxidant activity (mg GAE / mL extract)} = 10212.4\ (\text{mg GAE / mL extract}) + 813.3\ (\text{mg GAE / (mL extract}\cdot^{\circ}\text{C))}\cdot\text{A } (^{\circ}\text{C}) - 131.7\cdot(\text{mg GAE / (mL extract}\cdot\text{min))) B (min) - 1090.0 ((mg GAE / (mL extract}\cdot^{\circ}\text{C}\cdot\text{min})))}\cdot\text{A } (^{\circ}\text{C})\cdot\text{B (min)} + 2971.1\ (\text{mg GAE / (mL extract}\cdot^{\circ}\text{C}^2))\cdot\text{A}^2\ (^{\circ}\text{C}^2) \quad (2)$$

where TPC, A and B are the total polyphenol content, temperature and time of extraction, respectively.

In this way and after optimizing the obtained results, the values of 50 °C and 34.7 min for the extraction temperature and time, respectively, were selected as the optimal conditions to maximize both TPC and antioxidant activity.

3.1.2. *Effect of pepper:methanol ratio*

Once the optimal extraction conditions were defined (50 °C and 34.7 min), the best pepper:methanol ratio was evaluated (Table 2). Firstly, it was observed that an increase in the amount of pepper and methanol (although maintaining the substrate:solvent ratio) had a negative effect on both the TPC and the antioxidant activity (Table 2). This observation could be explained considering that when larger amounts of substrate and solvent are employed, they cannot interact properly, and, thus, the extraction process becomes less efficient. On the other hand, an increase in the amount of pepper (50, 100, 200, 400 g) maintaining the volume of methanol (100 mL), led to an improvement in the TPC. In contrast, TPC decreased when the amount of pepper was constant (100 g) and the volume of methanol was increased (50, 100, 200, 400 mL). In both cases,

Table 2
Total polyphenol content (TPC) and antioxidant activity of extracts obtained using different amounts of pepper and methanol (extracting solvent). Codes were used to model the parameters (−1: minimum value; 1: maximum value). Different letters indicate significant differences ($p < 0.05$).

Pepper (g)	Methanol (mL)	Ratio	Pepper code	Methanol code	TPC (mg GAE/mL extract)	Antioxidant activity (mg GAE/mL extract)
50	50	1/1	−1	−1	443.36^{a}	13924.67^{A}
100	100	1/1	−0.71	−0.71	361.32^{b}	$13,614.70^{A}$
200	200	1/1	−0.14	−0.14	316.55^{b}	12324.67^{B}
400	400	1/1	1	1	297.45^{bd}	11741.33^{C}
100	50	2/1	−0.71	−1	564.27^{c}	12801.33^{DF}
100	200	1/2	−0.71	−0.14	289.73^{d}	12534.67^{D}
100	400	1/4	−0.71	1	131.09^{e}	9578.00^{E}
50	100	1/2	−1	−0.71	308.82^{bd}	13088.00^{F}
200	100	2/1	−0.14	−0.71	557.00^{c}	12791.33^{DF}
400	100	4/1	1	−0.71	548.82^{c}	12161.33^{BD}

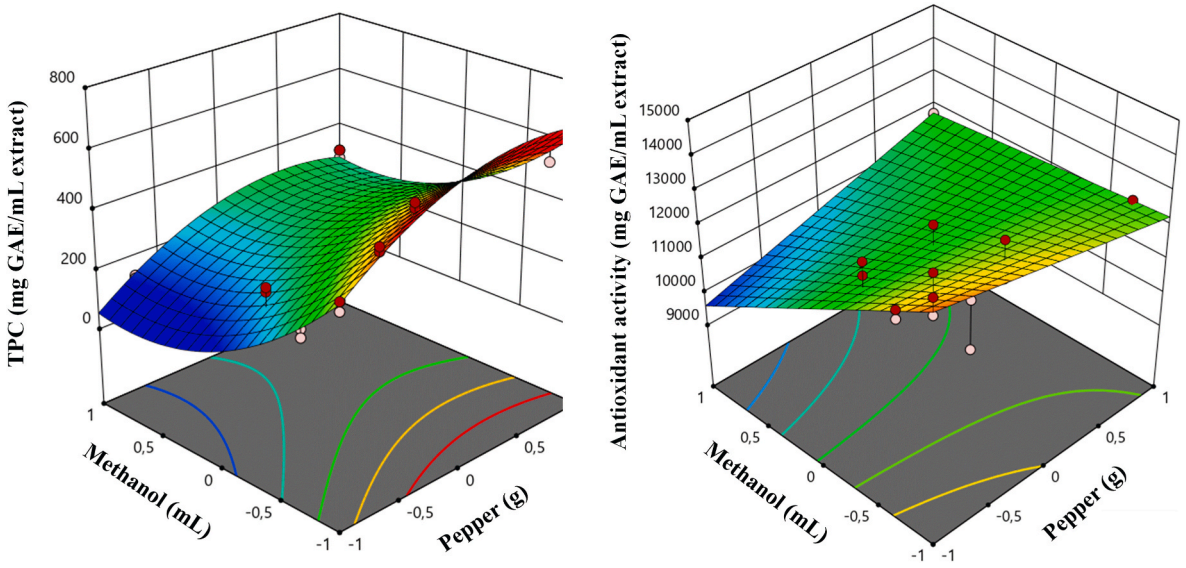

Fig. 2. Response surface of total polyphenol content (TPC) and antioxidant activity of extracts obtained using different amounts of pepper and methanol (extraction solvent). Pepper and methanol contents are codified from −1 to 1, being the minimum (50 g or mL) and maximum values (400 g or mL), respectively.

antioxidant activity did not seem to be significantly altered. In this way, it can be predicted that methanol has a great capacity to extract polyphenols from pepper as long as there is good interaction between pepper and methanol. Therefore, greater amounts of methanol do not contribute to enhancing polyphenols' extraction. On the contrary, they contribute to diluting the obtained extracts. Similar results were found in the literature (Galvan d'Alessandro et al., 2012).

Furthermore, in this case, a quadratic model could predict the TPC response. However, the antioxidant activity must be described with a two-factor interaction (2FI) model. Both models were represented in Eqs. (3) and (4), respectively, depending on the amounts of pepper (P) and methanol (M) used. Again, the lack of fit and the value of pure error indicated the good reproducibility of the experimental results (Table S2). The response surface generated by these models is shown in Fig. 2. TPC was quadratically affected by the amount of pepper and the volume of methanol to the same extent (similar exponents), although no significant interactions were found between them. On the contrary, these variables linearly affected antioxidant activity, with the effect of methanol being the most influential one (greatest exponent). Moreover, a strong synergistic effect between both variables was observed. The optimization of these independent variables to obtain the maximum TPC and antioxidant activity with the least amount of pepper and methanol possible was achieved with 89.1 g of pepper and 50 mL of methanol (pepper:methanol ratio 1.8:1).

$$\text{TPC (mg GAE / mL extract)} = 344.3\ (\text{mg GAE / mL extract}) + 115.8\ (\text{mg GAE / (mL extract·g pepper)})\cdot P\ (\text{g pepper}) - 197.5\ (\text{mg GAE / (mL extract·mL methanol)})\cdot M\ (\text{mL methanol}) - 115.1\ (\text{mg GAE / (mL extract·g pepper}^2))\cdot P^2\ (\text{g pepper}^2) + 139.1\ (\text{mg GAE / (mL extract·mL methanol}^2))\cdot M^2\ (\text{mL methanol}^2) \quad (3)$$

$$\text{Antioxidant activity (mg GAE / mL extract)} = 11864.4\ (\text{mg GAE / mL extract}) + 172.4\ (\text{mg GAE / (mL extract·g pepper)})\cdot P\ (\text{g}) - 1170.1\ (\text{mg GAE / (mL extract·mL methanol)})\cdot M\ (\text{mL methanol}) + 911.9\ (\text{mg GAE / (mL extract·g pepper·mL methanol)})\cdot P\ (\text{g pepper})\cdot M\ (\text{mL methanol}) \quad (4)$$

where TPC, P and M denote the total polyphenol content, the amounts of pepper and methanol, respectively.

3.1.3. Effect of extraction solvent

Apart from methanol, water and ethanol were evaluated as extraction solvents. For this purpose, the optimal temperature and time of extraction (50 °C and 34.7 min, respectively) and the optimal amounts of pepper and solvent (100 g of pepper and 50 mL of methanol; pepper: solvent ratio: 2:1) were used. Table 3 shows the TPC and antioxidant activity obtained with the different extraction solvents. Methanol was the best solvent for polyphenols' extraction, since it enabled the highest TPC. This result could be due to two effects. First, the higher polarity of the solvent improved polyphenol extraction, as was already reported by Do et al. (2014) (Do et al., 2014). On the other hand, all the polyphenolic groups have a great solubility in alcoholic solvents. The latter could be the reason why water, although having higher polarity than methanol, did not obtain the best TPC value, since condensed tannins, lignins and hydroxycinnamic acids (polyphenolic groups) cannot be dissolved in water, thus reducing the extraction yields of polyphenols in this solvent (Haminiuk et al., 2012). Regarding the antioxidant activity, its behavior was the opposite of that of TPC, although all solvents were able to extract polyphenols with high antioxidant activity (Table 3).

Table 3
Total polyphenol content (TPC) and antioxidant activity of extracts obtained using different extracting solvents and pepper parts. Different letters indicate significant differences ($p < 0.05$).

Extracting solvent	Pepper zone	TPC (mg GAE/mL extract)	Antioxidant activity (mg GAE/mL extract)
Methanol	Whole	564.7^{a}	12801.33^{A}
	Pulp	465.64^{b}	14951.33^{B}
	Waste	542.45^{a}	7878.00^{C}
Water		438.36^{b}	13994.67^{D}
Ethanol		398.36^{c}	15664.67^{B}

3.1.4. Effect of the pepper part employed for the extraction processes

The TPC and antioxidant activities from polyphenols extracted from different parts of the pepper (whole, pulp or waste) were also analyzed. For this purpose, the optimal temperature and time of extraction (50 °C and 34.7 min, respectively) and amounts of pepper and solvent (100 g of pepper and 50 mL of methanol) were used. The results displayed in Table 3 indicate that pepper waste had more polyphenol content than pepper pulp. However, the polyphenols found in the pulp had higher antioxidant activity than those found in the waste. This may be due to the time that these polyphenols have been in the plant, since the peduncle, seeds and pericarp (waste part) are the first parts to be formed in the pepper (Rylski, 2018).

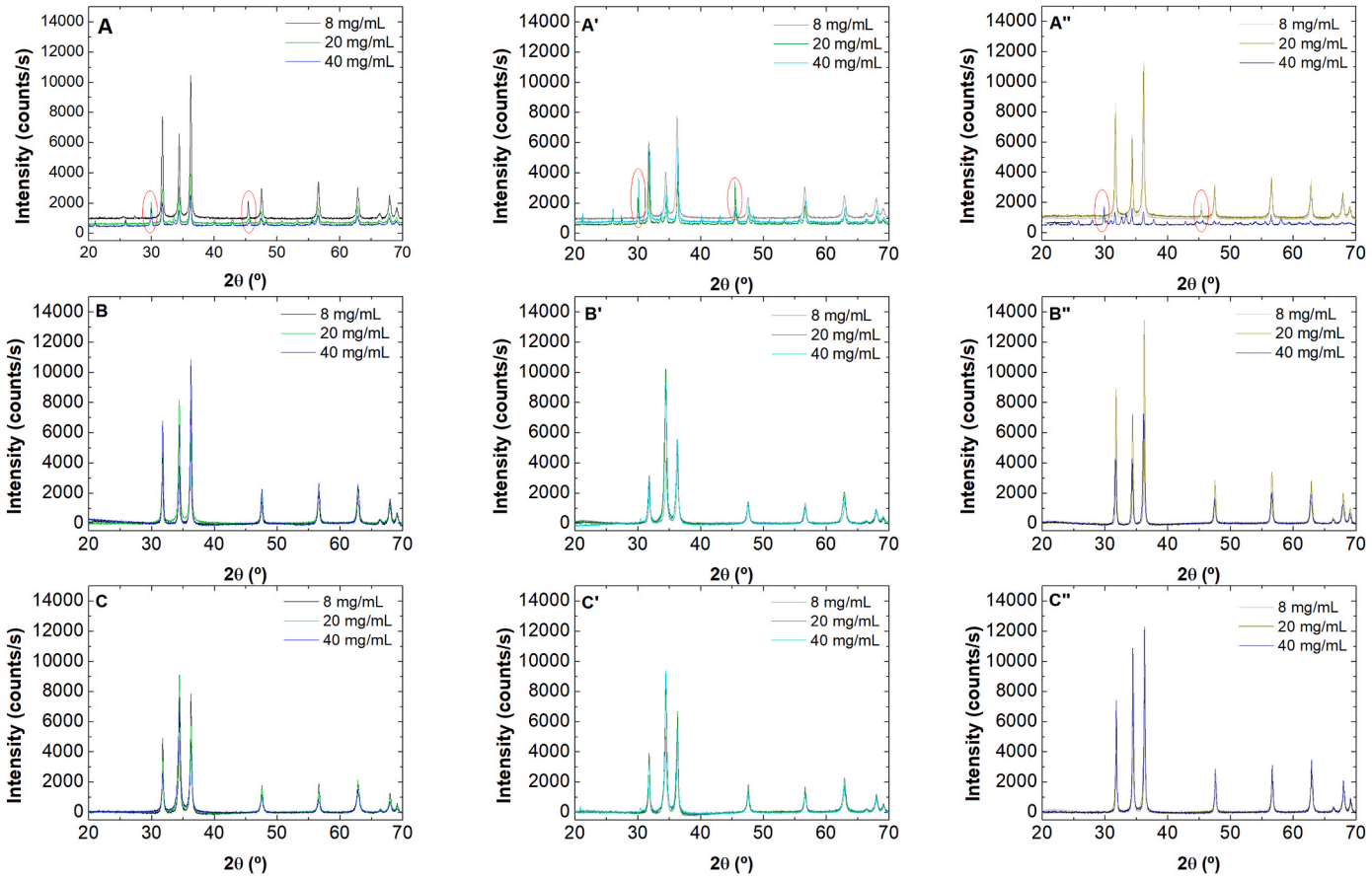

Fig. 3. XRD profiles of the ZnO nanoparticles obtained using chemical (A, A′ and A″), pepper polyphenols (B, B′ and B″) or pepper waste polyphenols (C, C′ and C″) as reducing agents at different precursor concentrations (8, 20 and 40 mg/mL) and precursor:reducing agent ratios [1:1 (A, B, C), 1:2 (A′, B′, C′) and 2:1 (A″, B″, C″)]. Red ovals indicate peaks at 2θ = 29.9 and 45.5°.

3.2. NPs synthesis

Once the polyphenol extraction process was optimized, NPs were synthesized. To this end, pepper and waste pepper extracts obtained with the optimal extraction conditions (50 °C and 34.7 min of mixing, 100 g of pepper and 50 mL of methanol) were used and compared with those chemically synthesized. The chemical process has a higher yield (70–85%) than the green one (1–5% in the case of pepper and 20–40% for pepper waste). Therefore, an optimization of the green NPs synthesis is still necessary to increase the yield of the process.

3.2.1. XRD

Fig. 3 shows the XRD pattern of all the synthesized NPs at different precursor concentrations and precursor:reducing agent ratio. All the profiles presented the nine characteristic peaks (2θ = 31.8, 34.5, 36.4, 47.7, 56.7, 62.9, 66.4, 68.0 and 69.1°) of hexagonal zincite ZnO (indexed by JCPDS Card No. 01-089-0510) (Jabeen et al., 2014). In turn, chemical NPs profiles showed other peaks (2θ = 29.9 and 45.5), which correspond to impurities due to the presence of NaOH during synthesis. These impurities were $NaZnCl_4{\cdot}H_2O$ and $Zn_2OCl_2{\cdot}H_2O$. In addition, the percentage of ZnO in the chemically synthesized NPs varied according to the precursor concentration ($ZnCl_2$) (higher concentrations led to lower purity) and precursor:reducing agent ratio (2:1 ratio led to the purest NPs) (Table 3). These impurities were not observed in the green NPs synthesized from polyphenols. This indicates a great advantage of green synthesis over chemical synthesis, since it enables the production of pure

Table 4
XRD parameters (ZnO percentage, crystallinity index and crystal size) of the ZnO nanoparticles obtained using chemical, pepper or pepper waste polyphenols as reducing agents at different precursor concentrations and precursor:reducing agent ratios. Different letters indicate significant differences ($p < 0.05$).

Number	Systems			ZnO percentage (%)			Crystallinity index (%)			XRD crystal size (nm)		
	Ratio	$ZnCl_2$ (mg/mL)	Reducing agent (mg/mL)	Chemical	Pepper	Pepper waste	Chemical	Pepper	Pepper waste	Chemical	Pepper	Pepper waste
1	1:1	8	8	86^{a}	100	100	83^{A}	80^{AB}	79^{B}	49^{α}	36^{γ}	$35^{\gamma\varepsilon}$
2		20	20	65^{b}	100	100	78^{B}	75^{BC}	78^{B}	46^{β}	30^{ε}	28^{ε}
3		40	40	55^{c}	100	100	77^{B}	70^{C}	76^{BC}	37^{γ}	$28^{\varepsilon\zeta}$	24^{ζ}
4	1:2	8	16	88^{a}	100	100	78^{B}	69^{CD}	61^{F}	$35^{\gamma\varepsilon}$	$29^{\varepsilon\zeta}$	40^{γ}
5		20	40	48^{d}	100	100	77^{B}	70^{C}	73^{C}	$48^{\alpha\beta}$	25^{ζ}	33^{ε}
6		40	80	36^{e}	100	100	77^{B}	71^{C}	77^{B}	52^{α}	26^{ζ}	27^{ε}
7	2:1	8	4	87^{a}	100	100	77^{B}	67^{D}	66^{D}	70^{δ}	38^{γ}	43^{γ}
8		20	10	93^{f}	100	100	81^{A}	77^{B}	79^{B}	51^{α}	36^{γ}	$35^{\gamma\varepsilon}$
9		40	20	37^{e}	100	100	80^{AB}	89^{E}	82^{A}	$47^{\alpha\beta}$	30^{ε}	32^{ε}

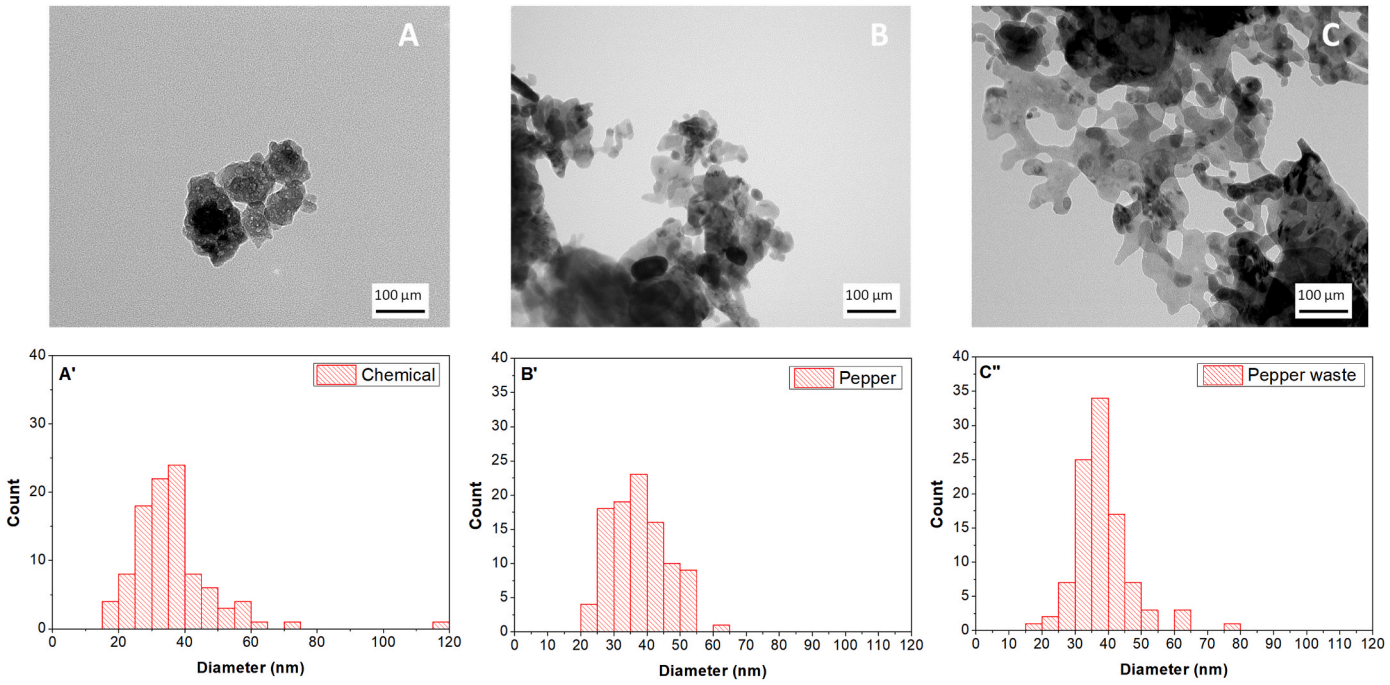

Fig. 4. TEM images and size distribution of the ZnO nanoparticles obtained using chemical (A and A′), pepper polyphenols (B and B′) or pepper waste polyphenols (C and C′) as reducing agents.

ZnO NPs (100% purity in the crystalline part, which is the one that can be analyzed with this technique).

Furthermore, the sharp diffraction peaks indicate the high crystallinity of the NPs. Consistently, all the NPs presented a crystallinity index greater than 60% (Table 4). However, no clear behavior patterns determined neither by the $ZnCl_2$ concentration nor by the ratios were observed. Regarding crystal size, the green method led to smaller NPs compared to the chemical method (24–43 and 35–70 nm for green and chemical NPs). Similar size were previously reported (Ahmed et al., 2017) by other polyphenol extracts, such as *Nephelium lappaceum* L. (25–40 nm), *L. lechenaultiana* (20–65 nm) or *Aloe vera* (25–40 nm). In addition, in general, the higher the $ZnCl_2$ concentration at the same $ZnCl_2$:reducing agent ratio, the smaller the NPs. Smaller NP sizes are very important, since they are often more active and show greater selectivity (Mudunkotuwa et al., 2012).

3.2.2. *TEM & EDS*

Chemically obtained NPs number 4 and green synthesized number 1

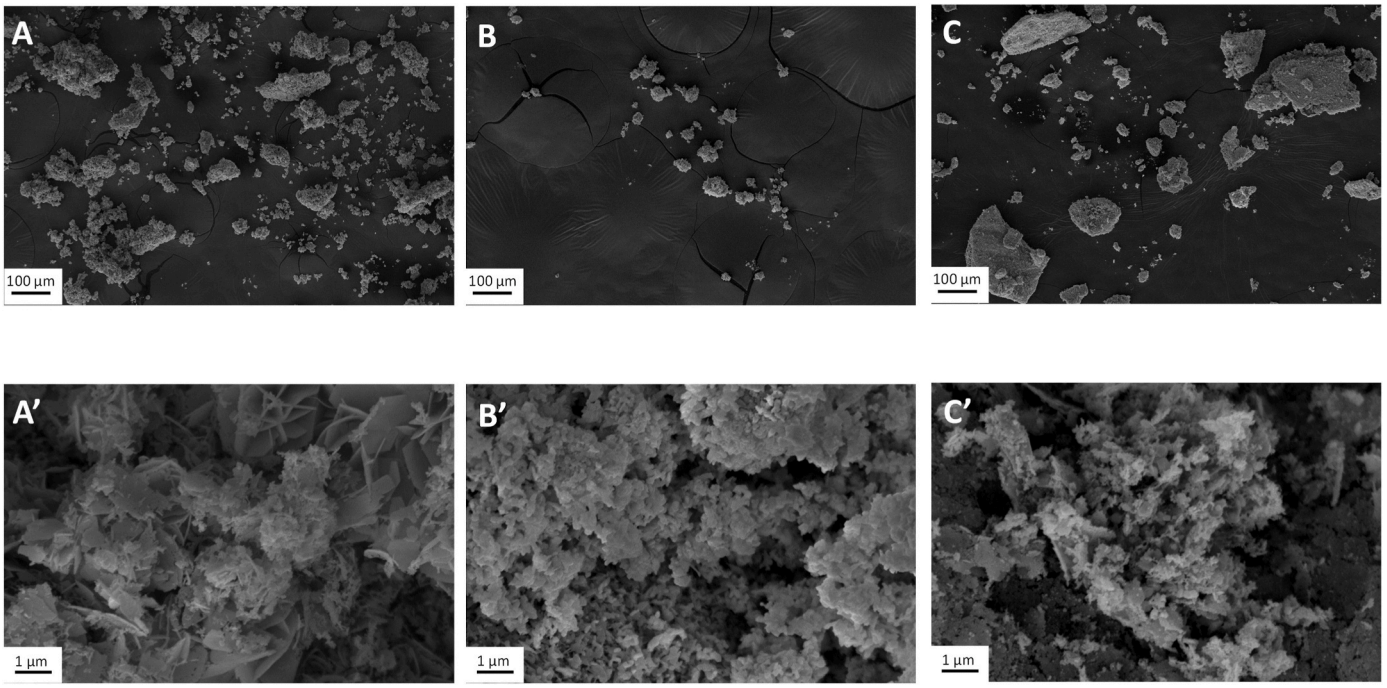

Fig. 5. SEM images and size distribution of the ZnO nanoparticles obtained using chemical (A, A′ and A″), pepper polyphenols (B, B′ and B″) or pepper waste polyphenols (C, C′ and C″) as reducing agents.

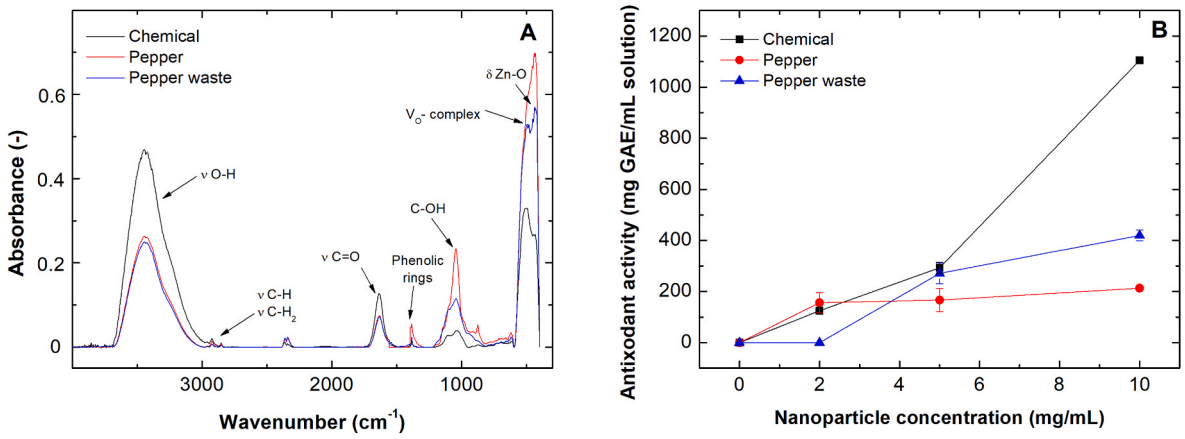

Fig. 6. FITR spectra (A) and antioxidant activity (B) of the ZnO nanoparticles obtained using chemical, pepper polyphenols or pepper waste polyphenols as reducing agents.

(pepper and pepper waste) were selected to compare the different methods of synthesis. This selection was carried out considering both their similar crystallinity index and crystal sizes. The microstructure of these NPs is shown in Fig. 4 (A, B and C for chemical, pepper and pepper waste NPs, respectively) as well as their size distribution (A′, B′ and C′ for chemical, pepper and pepper waste NPs, respectively). Chemically obtained NPs (Fig. 4A) had a rounder structure than the green ones (Fig. 4B and C), with the latter being heterogeneous spheres. Furthermore, although the mean size of NPs was similar in the three cases (consistently with those obtained by XRD), the size distribution was more heterogeneous for the chemically obtained NPs (Fig. 4A') than green ones (Fig. 4B' and 4C' for pepper and pepper waste respectively).

On the other hand, EDS analyses show that all the NPs present certain superficial contamination (5, 1 y 3 at.% for chemical, pepper and waste NPs, respectively). These can be assigned to residues of Cl (present in the precursor of the synthesis) and polyphenols (reductor agent in the green synthesis of NPs), who present peaks at the same energy. Thus, all NPs have >90 at.% purity, being purer the green ones (99 and 97% purity of pepper and pepper waste NPs, respectively, vs. 95% purity of chemical ones). As these compounds are generally amorphous, they could not be correctly identified by XRD, corresponding to the non-crystalline part identified in Table 4.

3.2.3. SEM

SEM images are shown in Fig. 5. The analysis of these images affirms the NP size distribution observed by TEM. In addition, the formation of aggregates formed by these NPs could also be observed. Although all the NPs formed aggregates, the smallest ones were those obtained from whole pepper NPs (13 ± 7 μm, Fig. 5B) and the largest ones, were those from pepper waste NPs (33 ± 8 μm, Fig. 5C). The formation of agglomerates of similar size was also reported in previous works (Benitez-Salazar et al., 2021).These results could be due to the lower antioxidant activity of the pepper waste polyphenols' extracts, which inhibits the surface tension of NPs to a lesser extent than those obtained from the whole pepper. In turn, chemically obtained NPs showed a medium aggregation (22 ± 20 μm, Fig. 5A), although with great dispersion, possibly due to the impurities present in their composition. Therefore, it can be concluded that the presence of the complex structures of polyphenols contributes to the functionalization of NPs, which would prevent aggregation. Nevertheless, polyphenols should retain their antioxidant activity (that is, not be degraded) to be able to transmit such property to the obtained NPs.

3.2.4. FTIR

Fig. 6A shows the FTIR profile of the selected NPs. All the samples presented the two characteristic peaks of ZnO NPs (Sharmila et al., 2019; Xiong et al., 2006): one at 505 cm^{-1}, associated with the oxygen vacancy defect complex (V_{O-} complex) in ZnO, and the other one, at 437 cm^{-1}, corresponding to the bending vibration of the Zn–O bond (δZn–O), being more pronounced in the green NPs. The presence of these latter bands demonstrates that the ZnO NPs have been successfully synthesized.

Besides these two bands, other absorption peaks were also observed and can be ascribed to vibrational modes associated with polyphenols or to the impurities remaining in the chemical synthesis, which were already observed in EDS analysis. The band at 3400 cm^{-1} can be attributed to the stretching mode of OH groups (νOH) present in the polyphenol extract and NaOH (Shigesato et al., 1988). The weak bands at 2900 and 2850 cm^{-1} arise from the stretching vibrational modes of the CH_2 and CH groups (νCH_2; νCH of aromatic rings in polyphenols), present in all the organic compounds, including polyphenols (Sivam et al., 2012). The band at 1625 can be ascribed to the stretching vibrational modes of carbonyl groups (νC = O) could correspond to the polysaccharides present in the peppers that have passed into the extract (Janaki et al., 2015), and also from moisture present in the samples. In turn, the bands at 1384 cm^{-1} arise from phenolic groups that remained in the NPs (Scano, 2021). Finally, the band at 1039 cm^{-1} can be attributed to C–OH bending (δCOH) from aromatic, secondary and tertiary alcohols, that is, OH groups attached to the phenolic groups and carbohydrates that may also have been extracted (Scano, 2021). As mentioned before, these compounds are generally amorphous, so they could not be correctly identified by XRD, corresponding to the non-crystalline part reported in Table 4.

Regarding the intermediate compounds (Fig. S1), the FTIR profile demonstrated the chemical reaction generated from polyphenols to form the intermediate hydroxide and this one, to form the final NPs. Thus, the peaks of these materials changed through the synthesis, being consistent with the synthesis reaction proposed above. Polyphenols generate an absorbance band between 1200 and 780 cm^{-1} that is generated by their aromatic rings (Grasel et al., 2016). These rings are consumed during the reaction, so they appear to a lesser extent in the intermediate components. On the other hand, the profile shown by the intermediate components confirms the formation of $Zn(OH)_2$. The peaks between 3400 and 3560 cm^{-1} are due to intermolecular hydrogen bonding (Davidov split) of the OH present in $Zn(OH)_2$. In addition, the peaks between 400 and 1100 cm^{-1} explain the stretching and bending bonds of the metal hydroxide (Parveen et al., 2010). These bands disappear when the hydroxide is calcined to get the oxide from the nanoparticles.

3.2.5. Antioxidant activity

The antioxidant activity of the selected NPs was evaluated as a function of NPs concentration (Fig. 6B). In general, an increase in the NPs concentration generated an increase in the antioxidant activity,

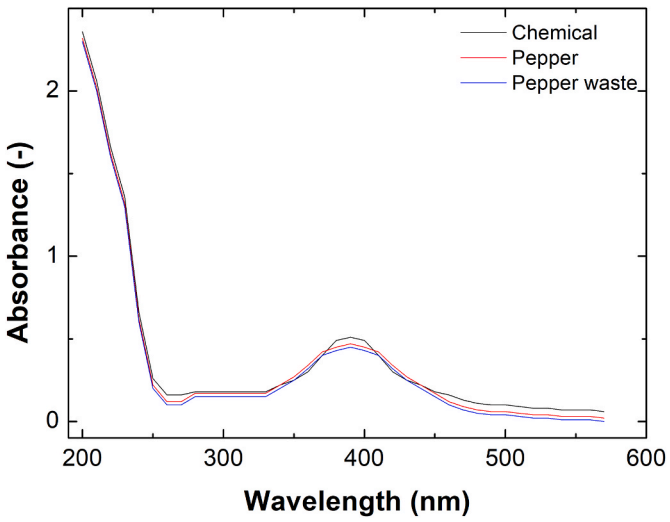

Fig. 7. UV–Vis spectra of the ZnO nanoparticles obtained using chemical, pepper polyphenols or pepper waste polyphenols as reducing agents.

except for NPs obtained using the whole pepper. In other words, a higher amount of NPs produced a higher catalytic surface that can interact with free radicals, improving the antioxidant function. It was also observed that chemically synthesized NPs had the highest antioxidant activity, followed by NPs obtained from pepper waste ones.

On the other hand, green synthesized NPs had a lower antioxidant capacity than the extracts used for their synthesis (Table 3). This is consistent, considering that part of this antioxidant capacity was used to reduce $ZnCl_2$ to form the ZnO NPs.

3.2.6. *Ultraviolet–visible (UV–Vis) spectroscopy*

UV–Vis spectra of the obtained NPs showed a band at 390 nm, characteristic of ZnO NPs (Fig. 7) (Dhanemozhi et al., 2017; Vennila and Jesurani, 2017). This peak arises from the plasmon resonance phenomenon (SPR) (Wang et al., 2021) and demonstrates the high purity of these materials. In addition, chemical NPs presented a narrower SPR band. This effect could be due to their lower purity demonstrated by XRD analyses. On the other hand, the band gap energy of the different NPs was obtained (Fig. S2). The linear part of $(A/\lambda)^2$ *vs.* $1/\lambda$ profile shows that the mode of transition in these NPs is direct in nature. The estimated band gap energy value of all the NPs was 3.1 eV, being consistent with the data obtained in bibliography (Bindu and Thomas, 2017). This value was lower than those obtained by bulk ZnO (3.37 eV) and could predict the best catalytic action of these NPs (Srikant and Clarke, 1997).

4. Conclusions

Polyphenols obtained from *Capsicum annuum* (pepper) could be used for the synthesis of NPs, leading to the production of more pure and cost-effective NPs using sustainable approaches. Furthermore, the use of pepper wastes as reducing agents represents a smart strategy to improve the circular economy. Nevertheless, there are some aspects to consider when synthesizing them, such as the method to extract the polyphenols and the precursor:reducing agent concentration and ratios used during the synthesis.

In this way, the green synthesis of NPs using pepper polyphenol extracts is a method that generated fewer impurities and toxic substances than chemical synthesis. In addition, this method gives added value to pepper waste, reducing its contamination, and enhancing the antioxidant functionality of the NPs without affecting their catalytic properties. These results support the future use of the obtained NPs in different applications, in the food and pharmaceutical fields.

CRediT authorship contribution statement

Mercedes Jiménez-Rosado: Conceptualization, Methodology, Formal analysis, Data curation, writing. **Andrea Gomez-Zavaglia:** Conceptualization, Methodology, Formal analysis, Validation, writing, Supervision. **Antonio Guerrero:** Validation, Resources, Funding acquisition. **Alberto Romero:** Conceptualization, Methodology, Validation, Resources, writing, Supervision.

Declaration of competing interest

The authors declare that they have no known competing financial interests or personal relationships that could have appeared to influence the work reported in this paper.

Acknowledgements

This work is a part of a research project supported by MCI/AEI/FEDER, EU (Ref. RTI2018-097100-B-C21) and Argentinean Agency for the Promotion of Scientific and Technological Promotion (PICT(2017)/1344 and PICT(2020)/0482). The authors gratefully acknowledge their financial support. In addition, the authors thank for the predoctoral grant of Mercedes Jiménez-Rosado (FPU17/01718, MEFP) and her research stay supported by Banco Santander. Andrea Gomez-Zavaglia is member of the Researcher Career CONICET (Argentinean Research Council). Finally, authors acknowledge the assistance in X-Ray and Microscopy services of CITIUS (University of Seville).

Appendix A. Supplementary data

Supplementary data to this article can be found online at https://doi.org/10.1016/j.jclepro.2022.131541.

References

Abdullah, J.A.A., Salah Eddine, L., Abderrhmane, B., Alonso-González, M., Guerrero, A., Romero, A., 2020. Green synthesis and characterization of iron oxide nanoparticles by pheonix dactylifera leaf extract and evaluation of their antioxidant activity. Sustain. Chem. Pharm. 17, 100280 https://doi.org/10.1016/j.scp.2020.100280.

Abomuti, M.A., Danish, E.Y., Firoz, A., Hasan, N., Malik, M.A., 2021. Green synthesis of zinc oxide nanoparticles using salvia officinalis leaf extract and their photocatalytic and antifungal activities. Biology 10, 1075. https://doi.org/10.3390/biology10111075.

Agarwal, H., Venkat Kumar, S., Rajeshkumar, S., 2017. A review on green synthesis of zinc oxide nanoparticles – an eco-friendly approach. Resour. Technol. 3, 406–413. https://doi.org/10.1016/j.reffit.2017.03.002.

Ahmed, S., Annu Chaudhry, S.A., Ikram, S., 2017. A review on biogenic synthesis of ZnO nanoparticles using plant extracts and microbes: a prospect towards green chemistry. J. Photochem. Photobiol. B Biol. 166, 272–284. https://doi.org/10.1016/j.jphotobiol.2016.12.011.

Almonacid, G.F., 2016. Evaluación de la variación del contenido de polifenoles en alimentos vegetales, en función del método de conservación empleado. Universidad Nacional de Cuyo.

Arthur Niamke, Michel, Soro, Soronikpoho, Tehi Sea, Bernard, Atchowo, Jaures Elidje, Djaman, Joseph Allico, 2021. Characterization of the physicochemical properties of sweet pepper (Capsicum annuum) cultivated in Korhogo in the North of Côte d'Ivoire. GSC Adv. Res. Rev. 8, 130–138. https://doi.org/10.30574/gscarr.2021.8.3.0204.

Benitez-Salazar, M.I., Niño-Castaño, V.E., Dueñas-Cuellar, R.A., Caldas-Arias, L., Fernández, I., Rodríguez-Páez, J.E., 2021. Chemical synthesis versus green synthesis to obtain ZnO powders: evaluation of the antibacterial capacity of the nanoparticles obtained by the chemical method. J. Environ. Chem. Eng. 9, 106544 https://doi.org/10.1016/j.jece.2021.106544.

Bindu, P., Thomas, S., 2017. Optical properties of ZnO nanoparticles synthesised from a polysaccharide and ZnCl 2. Acta Phys. Pol. A 131, 1474–1478. https://doi.org/10.12693/APhysPolA.131.1474.

Casagrande, M., Zanela, J., Wagner, A., Busso, C., Wouk, J., Iurckevicz, G., Montanher, P. F., Yamashita, F., Malfatti, C.R.M., 2018. Influence of time, temperature and solvent on the extraction of bioactive compounds of Baccharis dracunculifolia: in vitro antioxidant activity, antimicrobial potential, and phenolic compound quantification. Ind. Crop. Prod. 125, 207–219. https://doi.org/10.1016/j.indcrop.2018.08.088.

Chen, C.C., Liu, P., Lu, C.H., 2008. Synthesis and characterization of nano-sized ZnO powders by direct precipitation method. Chem. Eng. J. 144, 509–513. https://doi.org/10.1016/j.cej.2008.07.047.

Dawood, M., Oth, am I., Abali, A.M., 2020. Exploration of hidden fraudulent website dataset with different perspective. J. Comput. Theor. Nanosci. 17, 980–984. https://doi.org/10.1166/jctn.2020.8753.
Debnath, D., Gupta, A.K., 2018. Optimizing the fabrication of nano-plasmonic silver-nitrogen co-doped zinc oxide (Ag x Zn (1-x) N y O (1-y)) mediated by ammonia template: insight into its enhanced physiochemical and photocatalytic behavior. J. Mol. Liq. 249, 334–345. https://doi.org/10.1016/j.molliq.2017.11.050.
Dhanemozhi, A.C., Rajeswari, V., Sathyajothi, S., 2017. Green synthesis of zinc oxide nanoparticle using green tea leaf extract for supercapacitor application. Mater. Today Proc. 4, 660–667. https://doi.org/10.1016/j.matpr.2017.01.070.
Do, Q.D., Angkawijaya, A.E., Tran-Nguyen, P.L., Huynh, L.H., Soetaredjo, F.E., Ismadji, S., Ju, Y.-H., 2014. Effect of extraction solvent on total phenol content, total flavonoid content, and antioxidant activity of Limnophila aromatica. J. Food Drug Anal. 22, 296–302. https://doi.org/10.1016/j.jfda.2013.11.001.
de España, Gobierno, 2021. Web of Science [WWW Document]. Bioplastics Hortic. URL. https://apps.webofknowledge.com/WOS_GeneralSearch_input.do?product=WOS&search_mode=GeneralSearch&SID=C5IinIHhbtaoeqZWjry&preferencesSaved= (accessed 4.27.20).
Favre, L.C., Rolandelli, G., Mshicileli, N., Vhangani, L.N., dos Santos Ferreira, C., van Wyk, J., Buera, M. del P., 2020. Antioxidant and anti-glycation potential of green pepper (Piper nigrum): optimization of β-cyclodextrin-based extraction by response surface methodology. Food Chem. 316, 126280 https://doi.org/10.1016/j.foodchem.2020.126280.
Feijoo, S., González-García, S., Moldes-Diz, Y., Vázquez-Vázquez, C., Feijoo, G., Moreira, M.T., 2018. The environmental impact of magnetic nanoparticles under the perspective of carbon footprint. In: Environmental Carbon Footprints. Elsevier, pp. 45–77. https://doi.org/10.1016/B978-0-12-812849-7.00003-9.
Ferchichia, L., Chohraa, D., Mellouk, K., 2021. Total phenolic content, total flavonoid and antioxidant activity of methanolic and ethanolic extract of the flowers of a fruit tree cydoniablonga: quince from eastern Algeria. Ann. Rom. Soc. Cell Biol. 25, 1078–1087.
Food and Agriculture Organization of the United Nations, 2013. Food Wastage Footprint. Impacts on Natural Resources. FAO, Washington D.C.
Food and Agriculture Organization of the United Nations, 2021a. Presupuesto de nutrientes del suelo [WWW Document]. URL. http://www.fao.org/faostat/es/#data/QC/visualize (accessed 4.27.20).
Food and Agriculture Organization of the United Nations, 2021b. Data on Food and Agriculture [WWW Document]. URL. http://www.fao.org/ (accessed 10.13.19).
Galvan d'Alessandro, L., Kriaa, K., Nikov, I., Dimitrov, K., 2012. Ultrasound assisted extraction of polyphenols from black chokeberry. Separ. Purif. Technol. 93, 42–47. https://doi.org/10.1016/j.seppur.2012.03.024.
Gironi, F., Piemonte, V., 2011. Temperature and solvent effects on polyphenol extraction process from chestnut tree wood. Chem. Eng. Res. Des. 89, 857–862. https://doi.org/10.1016/j.cherd.2010.11.003.
Grasel, F., dos, S., Ferrão, M.F., Wolf, C.R., 2016. Development of methodology for identification the nature of the polyphenolic extracts by FTIR associated with multivariate analysis. Spectrochim. Acta Part A Mol. Biomol. Spectrosc. 153, 94–101. https://doi.org/10.1016/j.saa.2015.08.020.
Guozhong, C., 2004. Nanostructures and Nanomaterials: Synthesis, Properties and Applications. World Scientific Publishing Company, Singapur.
Haminiuk, C.W.I., Maciel, G.M., Plata-Oviedo, M.S.V., Peralta, R.M., 2012. Phenolic compounds in fruits - an overview. Int. J. Food Sci. Technol. 47, 2023–2044. https://doi.org/10.1111/j.1365-2621.2012.03067.x.
Handal, H.T., Mohamed, W.A.A., Labib, A.A., Moustafa, S.A., Sery, A.A., 2021. The influence of surface modification on the optical and capacitive properties of NiO nanoparticles synthesized via surfactant-assisted coprecipitation. J. Energy Storage 44, 103321. https://doi.org/10.1016/j.est.2021.103321.
Heiba, Z.K., Mohamed, M.B., Farag, N.M., Ahmed, S.I., 2021. Correlation between structural and optical characteristics upon changing the composition ratio of CuS@MnS nanocomposites. Appl. Phys. A 127, 281. https://doi.org/10.1007/s00339-021-04415-x.
INTA, Ministerio de Agricultura de Chile, 2018. Manual de pérdidas y desperdicios de alimentos. AL DÍA CHILE – INTA UNIVERSIDAD DE CHILE – MINISTERIO DE AGRICULTURA, Santiago de Chile.
Jabeen, M., Iqbal, M.A., Kumar, R.V., Ahmed, M., Javed, M.T., 2014. Chemical synthesis of zinc oxide nanorods for enhanced hydrogen gas sensing. Chin. Phys. B 23, 018504. https://doi.org/10.1088/1674-1056/23/1/018504.
Jamróz, E., Kulawik, P., Kopel, P., Balková, R., Hynek, D., Bytesnikova, Z., Gagic, M., Milosavlhevic, V., Adam, V., 2019. Intelligent and active composite films based on furcellaran: structural characterization, antioxidant and antimicrobial activities. Food Packag. Shelf Life 22, 100405. https://doi.org/10.1016/j.fpsl.2019.100405.
Janaki, A.C., Sailatha, E., Gunasekaran, S., 2015. Synthesis, characteristics and antimicrobial activity of ZnO nanoparticles. Spectrochim. Acta Part A Mol. Biomol. Spectrosc. 144, 17–22. https://doi.org/10.1016/j.saa.2015.02.041.
Kharazmi, S., Teheri-Kafrani, A., Soozanipour, A., 2020. Efficient immobilization of pectinase on trichlorotriazine-functionalized polyethylene glycol-grafted magnetic nanoparticles: a stable and robust nanobiocatalyst for fruit juice clarification. Food Chem., 126890 https://doi.org/10.1016/j.foodchem.2020.126890.
Leon, C.A., Roa-Morales, G., Martinez-Barrera, G., Menchaca-Campos, C., Bilyeu, B., Balderas-Hernandez, B., 2019. Sulfonated and gamma-irradiated waste expanded polystirene with iron oxide nanoparticles, for removal of indigo carmine dye in textile wastewater. Heliyon 15, e02071. https://doi.org/10.1016/j.heliyon.2019.e02071.
Li, C.-J., 2016. Reflection and perspective on green chemistry development for chemical synthesis—daoist insights. Green Chem. 18, 1836–1838. https://doi.org/10.1039/C6GC90029A.
Li, C.-J., Trost, B.M., 2008. Green chemistry for chemical synthesis. Proc. Natl. Acad. Sci. Unit. States Am. 105, 13197–13202. https://doi.org/10.1073/pnas.0804348105.
Mariano, M., El Kissi, N., Dufresne, A., 2014. Cellulose nanocrystals and related nanocomposites: review of some properties and challenges. J. Polym. Sci., Part B: Polym. Phys. 52, 791–806. https://doi.org/10.1002/polb.23490.
Marín, A., Ferreres, F., Tomás-Barberán, F.A., Gil, M.I., 2004. Characterization and quantitation of antioxidant constituents of sweet pepper (Capsicum annuum L.). J. Agric. Food Chem. 52, 3861–3869. https://doi.org/10.1021/jf0497915.
Mudunkotuwa, I.A., Rupasinghe, T., Wu, C.-M., Grassian, V.H., 2012. Dissolution of ZnO nanoparticles at circumneutral pH: a study of size effects in the presence and absence of citric acid. Langmuir 28, 396–403. https://doi.org/10.1021/la203542x.
Murty, B.S., Shankar, P., Raj, B., Rath, B.B., Murday, J., 2013. Unique properties of nanomaterials. In: Textbook of Nanoscience and Nanotechnology. Springer Berlin Heidelberg, Berlin, Heidelberg, pp. 29–65. https://doi.org/10.1007/978-3-642-28030-6_2.
Nematollahi, F., Konjini, F.T., Hergalani, F.Z., 2021. Determination of the antioxidant activity of calendula officinalis extract and its role in synthesis of ZnO nanoparticles. J. Food Technol. Nutr. 72, 127–134.
Nguyen, T.K.A., Kuncoro, E.P., Doong, R.-A., 2021. Manganese ferrite decorated N-doped polyacrylonitrile-based carbon nanofiber for the enhanced capacitive deionization. Electrochim. Acta, 139488. https://doi.org/10.1016/j.electacta.2021.139488.
Niora, M., Pedersbaek, D., Lassen, R.M.M., Weywadt, M.F. de V., Andresen, T.L., Simonsen, J.B., Jauffred, L., 2020. Head-to-head comparison of the penetration efficiency of lipid-based nanoparticles in a 3D tumor spheroid model. ChemRxiv 5, 21162–21171. https://doi.org/10.26434/chemrxiv.12136320.v1.
Noreen, H., Semmar, N., Farman, M., McCullagh, J.S.O., 2017. Measurement of total phenolic content and antioxidant activity of aerial parts of medicinal plant Coronopus didymus. Asian Pac. J. Trop. Med. 10, 792–801. https://doi.org/10.1016/j.apjtm.2017.07.024.
Özbek, H.N., Halahlih, F., Göğüş, F., Koçak Yanık, D., Azaizeh, H., 2020. Pistachio (Pistacia vera L.) Hull as a potential source of phenolic compounds: evaluation of ethanol–water binary solvent extraction on antioxidant activity and phenolic content of Pistachio Hull extracts. Waste Biomass Valoriz. 11, 2101–2110. https://doi.org/10.1007/s12649-018-0512-6.
Parveen, M.F., Umapathy, S., Dhanalakshmi, V., Anbarasan, R., 2010. Synthesis and characterization of nano-sized Zn(OH)2 and Zn(OH)2/PVA nano-composite. Compos. Interfac. 17, 757–774. https://doi.org/10.1163/092764410X519417.
Parveen, K., Banse, V., Ledwani, L., 2016. Green synthesis of nanoparticles: their advantages and disadvantages. In: AIP Conference Proceedings. AIP Conference Proceedings, 020048. https://doi.org/10.1063/1.4945168.
Pérez-Labrada, F., Hernández-Hernández, H., López-Pérez, M.C., González-Morales, S., Bernavides-Mendoza, A., Juárez-Maldonado, A., 2020. Nanoparticles in plants: morphophysiological, biochemical and molecular responses. In: Plant Life under Changing Environment. ELsevier, Paises Bajos, pp. 289–322. https://doi.org/10.1016/B978-0-12-818204-8.00016-3.
Petcharoen, K., Sirivat, A., 2012. Synthesis and characterization of magnetite nanoparticles via the chemical co-precipitation method. Mater. Sci. Eng. B 177, 421–427. https://doi.org/10.1016/j.mseb.2012.01.003.
Pietrzak, W., Nowak, R., Olech, M., 2014. Effect of extraction method on phenolic content and antioxidant activity of mistletoe extracts from Viscum album subsp. abietis. Chem. Pap. 68, 976–982. https://doi.org/10.2478/s11696-013-0524-4.
Pourrahimi, A.M., Liu, D., Pallon, L.K.H., Andersson, R.L., Martínez Abad, A., Lagarón, J.-M., Hedenqvist, M.S., Ström, V., Gedde, U.W., Olsson, R.T., 2014. Water-based synthesis and cleaning methods for high purity ZnO nanoparticles – comparing acetate, chloride, sulphate and nitrate zinc salt precursors. RSC Adv. 4, 35568–35577. https://doi.org/10.1039/C4RA06651K.
Prabhu, S., Poulose, E.K., 2012. Silver nanoparticles: mechanism of antimicrobial action, synthesis, medical applications, and toxicity effects. Int. Nano Lett. 2, 32. https://doi.org/10.1186/2228-5326-2-32.
Prado, J.M., Vardanega, R., Debien, I.C.N., Meireles, M.A.A., Gerschenson, L.N., Sowbhagya, H.B., Chemat, S., Prado, J.M., Vardanega, R., Debien, I.C.N., Meireles, M.A.A., Gerschenson, L.N., Sowbhagya, H.B., Chemat, S., 2021. Conventional extraction. In: Food Waste Recovery. Elsevier, London, pp. 109–127. https://doi.org/10.1016/B978-0-12-820563-1.00015-9.
R, N.A., I, W.R.W., 2012. Evaluation of polyphenol content and antioxidant activities of some selected organic and aqueous extracts of cornsilk (Zea mays Hairs). J. Med. Bioeng. 1, 48–51. https://doi.org/10.12720/jomb.1.1.48-51.
Rajeswari, V.D., Khalifa, A.S., Elfasakhany, A., Badruddin, I.A., Kamangar, S., Brindhadevi, K., 2021. Green and ecofriendly synthesis of cobalt oxide nanoparticles using Phoenix dactylifera L: antimicrobial and photocatalytic activity. Appl. Nanosci. https://doi.org/10.1007/s13204-021-02038-5.
Rylski, I., 2018. Pepper (Capsicum). In: Handbook of Fruit Set and Development. CRC Press, Boca Raton, pp. 341–354.
Saleem, S., Hasnain Jameel, M., Akhtar, N., Nazir, N., Ali, A., Zaman, A., Rehman, A., Butt, S., Sultana, F., Mushtaq, M., Hui Zeng, J., Amami, M., Althubeiti, K., 2021. Modification in structural, optical, morphological, and electrical properties of zinc oxide (ZnO) nanoparticles (NPs) by metal (Ni, Co) dopants for electronic device applications. Arab. J. Chem., 103518 https://doi.org/10.1016/j.arabjc.2021.103518.
Saleh, T.A., 2020. Nanomaterials: classification, properties, and environmental toxicities. Environ. Technol. Innovat. 20, 101067 https://doi.org/10.1016/j.eti.2020.101067.
Scano, P., 2021. Characterization of the medium infrared spectra of polyphenols of red and white wines by integrating FT IR and UV–Vis spectral data. LWT (Lebensm.-Wiss. & Technol.) 147, 111604. https://doi.org/10.1016/j.lwt.2021.111604.

Shankar, S., Rhim, J.-W., 2019. Effect of Zn salts and hydrolyzing agents on the morphology and antibacterial activity of zinc oxide nanoparticles. Environ. Chem. Lett. 17, 1105–1109. https://doi.org/10.1007/s10311-018-00835-z.

Sharmila, G., Thirumarimurugan, M., Muthukumaran, C., 2019. Green synthesis of ZnO nanoparticles using Tecoma castanifolia leaf extract: characterization and evaluation of its antioxidant, bactericidal and anticancer activities. Microchem. J. 145, 578–587. https://doi.org/10.1016/j.microc.2018.11.022.

Sheldon, R.A., 2005. Green solvents for sustainable organic synthesis: state of the art. Green Chem. 7, 267. https://doi.org/10.1039/b418069k.

Shigesato, Y., Murayama, A., Kamimori, T., Matsuhiro, K., 1988. Characterization of evaporated amorphous WO3 films by Raman and FTIR spectroscopies. Appl. Surf. Sci. 33–34, 804–811. https://doi.org/10.1016/0169-4332(88)90384-4.

Sivam, A.S., Sun-Waterhouse, D., Perera, C.O., Waterhouse, G.I.N., 2012. Exploring the interactions between blackcurrant polyphenols, pectin and wheat biopolymers in model breads; a FTIR and HPLC investigation. Food Chem. 131, 802–810. https://doi.org/10.1016/j.foodchem.2011.09.047.

Spigno, G., Tramelli, L., De Faveri, D.M., 2007. Effects of extraction time, temperature and solvent on concentration and antioxidant activity of grape marc phenolics. J. Food Eng. 81, 200–208. https://doi.org/10.1016/j.jfoodeng.2006.10.021.

Srikant, V., Clarke, D.R., 1997. Optical absorption edge of ZnO thin films: the effect of substrate. J. Appl. Phys. 81, 6357–6364. https://doi.org/10.1063/1.364393.

Talam, S., Karummuri, S.R., Gunnam, N., 2012. Synthesis, characterization and spectroscopic properties of ZnO nanoparticles. Int. Sch. Res. Netw. 2012, 372505 https://doi.org/10.5402/2012/372505.

Tang, C., He, Z., Liu, Hongmei, Xu, Y., Huang, H., Yang, G., Xiao, Z., Li, S., Liu, Hongna, Deng, Y., Chen, Z., Chen, H., He, N., 2020. Application of magnetic nanoparticles in nucleic acid detection. J. Nanobiotechnol. 18, 62. https://doi.org/10.1186/s12951-020-00613-6.

Trost, B., 1991. The atom economy—a search for synthetic efficiency (80-.). Science 254, 1471–1477. https://doi.org/10.1126/science.1962206.

UNE-CEN ISO/TS 80004-2:2017, 2017. Nanotecnologías. Vocabulario. Parte 2. Nano-objetos.

Varma, R.S., 2012. Greener approach to nanomaterials and their sustainable applications. Curr. Opin. Chem. Eng. 1, 123–128. https://doi.org/10.1016/j.coche.2011.12.002.

Vennila, S., Jesurani, S.S., 2017. Eco-friendly green synthesis and characterization of stable ZnO Nanoparticle using small Gooseberry fruits extracts. Chemtech 10, 271–275.

Vijayalaxmi, S., Jayalakshmi, S.K., Sreeramulu, K., 2015. Polyphenols from different agricultural residues: extraction, identification and their antioxidant properties. J. Food Sci. Technol. 52, 2761–2769. https://doi.org/10.1007/s13197-014-1295-9.

Vivekananth, G.G., Poonkothai, M., Alaguprathana, M., 2021. Sustainable root mediated synthesis of iron oxide nanoparticles from Glycyrrhiza glabra and its environmental applications. SPAST Abstr. 1, 1.

Wang, Y., Zhang, M., Ma, H., Su, H., Li, A., Ruan, W., Zhao, B., 2021. Surface plasmon resonance from gallium-doped zinc oxide nanoparticles and their electromagnetic enhancement contribution to surface-enhanced Raman scattering. ACS Appl. Mater. Interfaces 13, 35038–35045. https://doi.org/10.1021/acsami.1c05804.

Wrona, M., Nerin, C., 2020. Analytical approaches for analysis of safety of modern food packaging: a review. Molecules 25, 752. https://doi.org/10.3390/molecules25030752.

Xiong, G., Pal, U., Serrano, J.G., Ucer, K.B., Williams, R.T., 2006. Photoluminescence and FTIR study of ZnO nanoparticles: the impurity and defect perspective. Phys. Status Solidi 3, 3577–3581. https://doi.org/10.1002/pssc.200672164.